Multifunctioning pH-Responsive Nanoparticles from Hierarchical Self-Assembly of Polymer Brush for Cancer Drug Delivery

Youqing Shen, Yihong Zhan, Jianbin Tang, Peisheng Xu, Patrick A. Johnson, and Maciej Radosz
Dept. of Chemical and Petroleum Engineering, Soft Materials Laboratory, University of Wyoming, Laramie, WY 82071

Edward A. Van Kirk and William J. Murdoch
Dept. of Animal Science, University of Wyoming, Laramie, WY 82071

DOI 10.1002/aic.11600
Published online September 23, 2008 in Wiley InterScience (www.interscience.wiley.com).

Polymer nanoparticles are extensively explored as drug carriers but they generally have issues of premature burst drug release, slow cellular uptake, and retention in acidic intracellular compartments. Herein, we report multifunctioning three-layered nanoparticles (3LNPs) that can overcome these problems. The 3LNPs have a poly(ε-caprolactone) (PCL) core, a pH-responsive poly[2-(N,N-diethylamino)ethyl methacrylate](PDEA) middle layer and a polyethylene glycol (PEG) outer layer. The pH-responsive PDEA layer is insoluble at pH above 7 but becomes positively charged and soluble via protonation at pH lower than 6.5. Thus, this layer has three functions: it covers on the PCL core inhibiting the premature burst drug release at the physiological pH, becomes positively charged and thus promotes endocytosis for fast cellular internalization in the acidic interstitium of solid tumors, and is highly positively charged in lysosomes to disrupt the lysosomal membrane and release the nanoparticle into the cytosol. The multifunctioning nanoparticles are an efficient carrier for cancer cytosolic drug delivery.
 AIChE J, 54: 2979–2989, 2008
Keywords: nanoparticles, pH-sensitive, self-assembly, polymer brush, drug delivery

Introduction

Polymer nanoparticles offer a suitable means to deliver various drugs to cancer tissues or cells.[1–6] Nanoparticles with long blood-circulation times, so called "stealth nanoparticles", can be fabricated from micelles formed by self-assembly of amphiphilic copolymers.[7,8] Such nanoparticles have a core-shell structure. The hydrophilic shell [usually a dense layer of polyethylene glycol (PEG) chains] evades the immune recognition[9,10] to have a long blood circulation time for passive accumulation into tumor tissues through their leaky blood capillaries, which is referred to as the enhanced permeability and retention effect.[9–12] The hydrophobic inner core can carry various anticancer drugs such as cisplatin,[13–17] doxorubicin,[18–22] paclitaxel,[23,24] camptothecin (CPT),[25,26] and etoposide.[27]

The premature (within the first several hours) burst drug release of most of the carried drug, however, is a general problem of nanoparticles.[28,29] Upon intravenous administration, the burst release corresponds to a nontargeted drug release which may lead to systemic toxicity as well as less drug availability to cancer tissues. The burst release could be

Correspondence concerning this article should be addressed to Y. Shen at sheny@uwyo.edu.

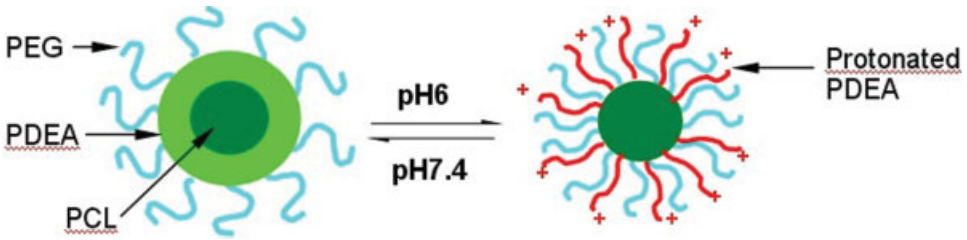

Scheme 1. The pH-responsive three-layered nanoparticles (3LNPs).

[Color figure can be viewed in the online issue, which is available at www.interscience.wiley.com.]

suppressed by covalently binding drugs to the core-forming polymers. For example, DOX was anchored to PLGA with a terminal COOH group[30] or grafted to poly(aspartic acid).[31] Such nanoparticles, however, showed low or completely no anticancer activity because chemically-attached DOX could not be released.[32–36]

Other common problems for most nanoparticles are their slow cellular internalization and lysosomal sequestration. Cytosolic drug release can overcome/bypass the overexpressed membrane-associated multidrug resistance of cancer cells.[22,32–37] This requires the nanoparticles to be able to rapidly enter the cells and quickly escape from the lysosomes to the cytoplasm. The cellular uptake of stealth nanoparticles, however, is generally slow due to the steric repulsion to the cells of their PEG layers.[38–40] Furthermore, these nanoparticles are retained in several cytoplasmic organelles mainly lysosomes after internalized.[41] Drug release into lysosomes, which have an acidic pH (~4–5) and various enzymes,[42,43] causes drug sequestration in the acidic compartments and drug degradation.[44,45]

Stimuli-responsive nanoparticles responding to tumor's properties have been developed to solve those problems. Solid tumors have an extracellular pH of typically about 7.06 with a range of 5.7–7.8.[46] Drug resistant cancer cells also often exhibit an altered pH-gradient across different cell compartments to increase the drug-sequestering capacity of the compartments, particularly more acidic recycling endosomes, lysosomes, Golgi, and mitochondria, but more basic cytosol and nucleus. Typically, the pH of late endosomes is near 5[47,48] and that of lysosomes is about 4–5.[42,43,49] Thus, the acidity of the tumor extracellular fluid was used as a trigger to expose the targeting groups[50] or generate positive charges[37] on the nanoparticle surface to promote endocytosis for fast cellular uptake. The lysosomal pH was used to regenerate positive charges of the nanoparticles to disrupt the lysosomal membrane for nanoparticle escape.[37]

We herein report a three-layered onion-structured nanoparticle responding to the solid tumor extracellular and lysosomal acidities to overcome the burst drug release, slow cellular uptake and lysosome escape problems for efficient cytosolic cancer drug delivery (Scheme 1). The nanoparticle has a hydrophobic poly(ε-caprolactone) (PCL) core for carrying drugs, a pH-responsive middle layer and a PEG outer layer. The pH-responsive middle layer is hydrophobic and collapses on the core at the physiological pH (7.4) to prevent the premature burst drug-release, but it becomes positively charged and protrudes out at the solid-tumor interstitial pH. This positively charged layer leads the nanoparticle to be adsorbed onto the negatively-charged cell membrane and subsequently induces adsorptive endocytosis of the nanoparticle. Once internalized and transferred to a lysosome, the poly[2-(N,N-diethylamino)ethyl methacrylate] (PDEA) layer is further charged, disrupting the lysosomal membrane to release the nanoparticles into the cytosol.

Experimental Section

Materials

Poly(ethylene glycol) methyl ether methacrylate macromonomer (mPEG, molecular weight (M_n) = 2000, polydispersity index (PDI) = 1.2) from Aldrich as 50% solution in water was dried using a rotary evaporator at room temperature under high vacuum. ε-Caprolactone (ε-CL) (Aldrich) and 2-(*N*,*N*-diethylamino)ethyl methacrylate (DEA) (Aldrich) were dried over calcium hydride. 2-Ethanol amine (Aldrich) was dried over molecular sieves. Tetrahydrofuran (THF) was distilled over benzophenone-sodium prior to use. CPT was purchased from Natland International Corporation, NC, USA. MTT cell proliferation assay kits were from American Type Culture Collection (ATCC). All other chemicals were purchased form Aldrich and used without further purification. Polycaprolactone methacrylate-macromonomer (mPCL, M_n = 3000, PDI = 1.4) was synthesized according to literature.[51]

Instrumentation

Gel permeation chromatography (GPC) was used to determine polymer molecular weights and polydispersity index. The measurements were operated on a Waters SEC equipped with a Waters 2414 refractive index detector, a laser light scattering detector (Precision Detectors, MA) and two 300-mm Solvent-Saving GPC columns (molecular weight ranges: 5×10^2–3×10^4 and 5×10^3–6×10^5) at a flow rate of 0.30 ml/min using THF as solvent at 30°C. Data were recorded and processed with the Waters software package. ^{1}H-NMR spectra were recorded on a Bruker Avance DRX-400 spectrometer using $CDCl_3$ as solvent. Chemical shifts were reported downfield from 0.00 ppm using tetramethylsilane as internal reference. The sizes of the micelles were determined using a Nano-ZS Nanosizer (Malvern Instrument, UK) with a laser light wavelength of 632.8 nm and a scattering angle at 173°. The zeta potentials of the micelles were determined using phase analysis light scattering technology using the Nano-ZS Nanosizer routinely calibrated with a −50-mV zeta

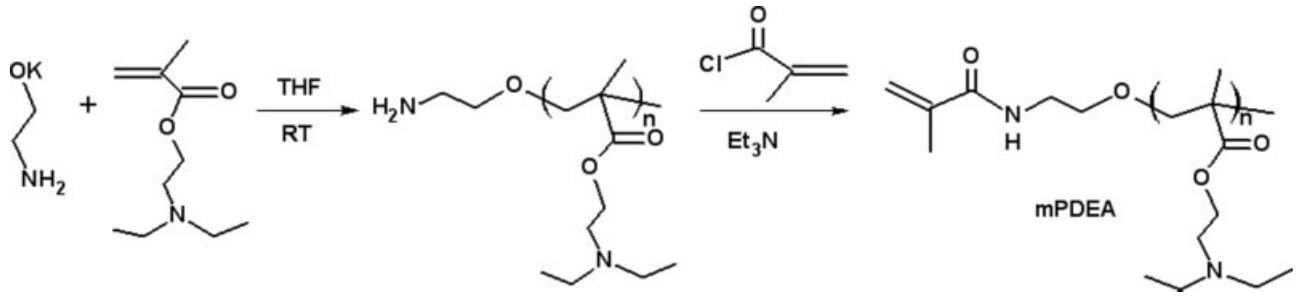

Scheme 2. Synthesis of PDEA macromonomer (mPDEA).

potential standard solution (Malvern Instruments). The morphology of the nanoparticles was observed using a Hitachi H-7000 transmission electron microscope (TEM) at an acceleration voltage of 75 kV. The adsorption onto the cell membrane and the endocytosis of the nanoparticles were observed using a Leica TCS SP2 Confocal Microscope. The endocytosis of the nanoparticles was further quantitated using flow cytometry (NPE SYSTEMS, Pembroke Pines, FL, USA).

Synthesis of PDEA macromonomer (Scheme 2)

A typical synthesis procedure is as follows: A dried 100-ml round-bottomed flask was degassed by vacuum/nitrogen purging and heating for three cycles. Dried THF (20 ml) was added via a dry syringe. Dried 2-ethanolamine (0.121 ml, 2 mmol) was added. Potassium naphthalene (2 mmol) in THF was then added. The mixture solution was stirred at room temperature for several minutes to form the alcoholate initiator. Freshly dried DEA monomer (6 ml, 30 mmol) was added quickly. The anionic polymerization was conducted at room temperature for 5 h before adding a small amount of methanol to terminate the reaction. The product was purified by repeated precipitation in cold n-hexane. The oily polymer (PDEA) was isolated in a yield of 93.4%. The molecular weight of the resulting PDEA had a M_n of 2.5 KDa and a PDI of 1.3.

The ω-amino-PDEA (M_n, 2.5 KDa) reacted with methacryloyl chloride to form PDEA macromonomer (mPDEA). The reaction was performed under dry nitrogen. Dried CH_2Cl_2 (60 ml) and triethylamine (1.95 ml, 14 mmol) were added via dry syringes to a 100-ml round-bottomed flask containing ω-amino-PDEA (10 g, 4 mmol). Methacryloyl chloride (1.25 g, 12 mmol) in CH_2Cl_2 was added dropwise to the solution. The reaction was kept at 0°C for 2 h and then at room temperature overnight. The solution was filtered to remove the salt. The CH_2Cl_2 solution was washed with water for several times and finally precipitated in cold n-hexane. The oily product was isolated (yield: 57.8%) and dried under vacuum. ^{1}H NMR ($CDCl_3$): δ 6.24 (CH_2=CCH_3), 5.83 (CH_2=$C(CH_3)$—), 4.01 ($COOCH_2CH_2$), 2.68 ($COOCH_2CH_2N$), 2.54 (NCH_2CH_3), 1.94 (—$CH_2(CH_3)COO$), 1.03 (—(CH_3)COOC, NCH_2CH_3).

Synthesis of the brush terpolymer by macromonomer copolymerization (Scheme 3)

The brush terpolymer was synthesized by free radical copolymerization as we reported.[51] mPCL (M_n = 3.0 KDa, 2.0 g, 0.6 mmol), mPEG (M_n = 2.1 KDa, 1.25 g, 0.6 mmol), mPDEA (M_n = 2.5 KDa, 1.52 g, 0.6 mmol), and AIBN (60 mg) were charged in a Schlenk tube. The tube was sealed and degassed by vacuum/nitrogen purging for three cycles. Degassed DMF (5 ml) was added via a syringe. The mixture was heated in an 80°C oil bath. At timed intervals, the reaction solution (0.05 ml) was taken using degassed syringes. The progress of the polymerization and the resulting polymer molecular weight and PDI were measured by GPC.[51] Finally, the reaction mixture was precipitated in 10-fold methanol and dialyzed against DI water (MWCO = 12,000) to remove the unreacted mPEG. The final product was isolated in a yield of 43.9% and dried under vacuum for 48 h. The PCL/PDEA/PEG had M_n of 10.8 KDa with a PDI of 1.8. ^{1}H NMR ($CDCl_3$): 4.05 [$COOCH_2CH_2N$, $COOCH_2(CH_2)_4$], 3.62 (—OCH_2CH_2O), 2.71 (—$CH_2COOCH_2CH_2$), 2.58 ((NCH_2-CH_3), 2.30 ($OOCCH_2(CH_2)_4O$), 1.94 ($CH_2(CH_3)COO$), 1.65 ($OOCCH_2CH_2(CH_2)_3O$), 1.38 ($OOC(CH_2)_2CH_2(CH_2)_2O$), 1.25 ((CH_3)$_2$CHO), 1.03 ($COOC(CH_3)$, NCH_2CH_3). The PCL/PDEA/PEG chain ratio measured with ^{1}H-NMR by the inten-

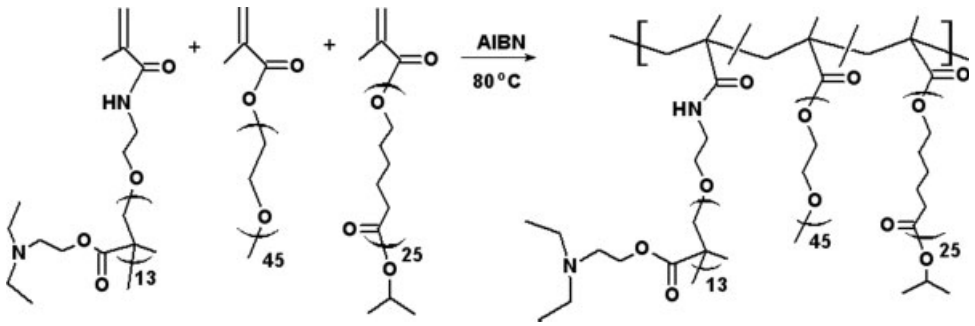

Scheme 3. Preparation of the terpolymer brush via macromonomer copolymerization.

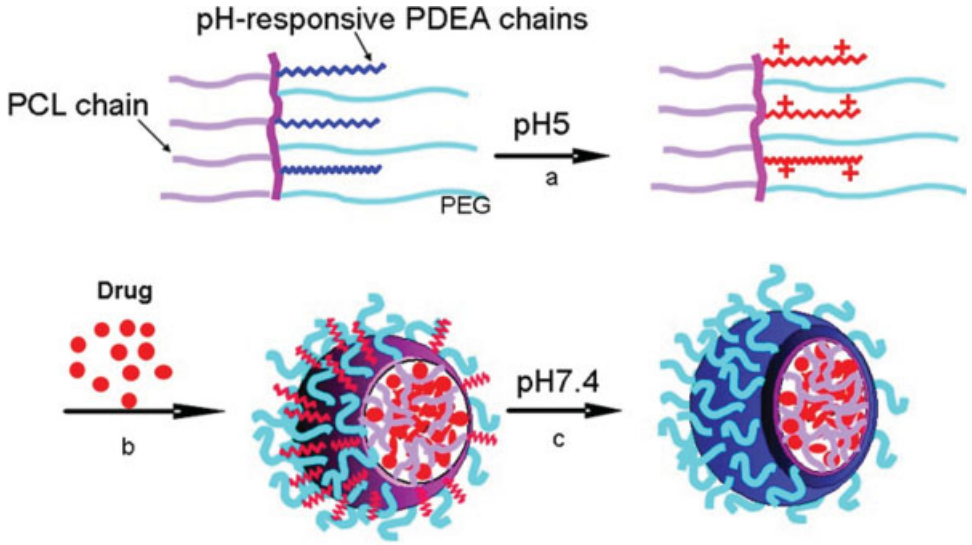

Scheme 4. Fabrication of drug-loaded pH-responsive three-layered onion structured nanoparticles via pH-controlled hierarchical self-assembly (two-step method).

[Color figure can be viewed in the online issue, which is available at www.interscience.wiley.com.]

sity ratio of the CH_2 signal in PEG (OCH_2CH_2, 3.62 ppm), PCL (CH_2COO, 2.30 ppm), and CH_3 signal in PDEA (NCH_2CH_3, 1.03 ppm) was 0.90:1.0:1.9.

Nanoparticle fabrication

(a) Two-step method (Scheme 4): The copolymer (2.5 mg) was dissolved in 1 ml of acetone with stirring. The acetone solution was dropwise added into 5 ml of deionized water at pH 5 with stirring. The solution pH was measured after the addition of the acetone solution and adjusted to pH 5 using diluted HCl if the pH changed. The solution was stirred for 30 min and then the pH was raised to 7.4 by adding Na_2CO_3 solution. The solution was stirred under reduced pressure for 12 h to remove the acetone.

(b) One-step method: In the above method, polymer-acetone solution was simply added dropwise into 5 ml of deionized water without adjusting the pH, and then the solution was stirred under reduced pressure for 12 h to remove the acetone.

Loading CPT into the nanoparticles

CPT was loaded into the nanoparticles using the two or one step-method from 1 ml of acetone solution containing terpolymer (2.5 mg) and CPT (0.5 mg). After acetone was removed, the solution was filtered through a 450-nm syringe filter to remove the free CPT. To determine the CPT content, 0.1 ml of the nanoparticle solution was dried and the nanoparticles were dissolved in DMSO. The CPT concentration in the DMSO solution was determined by UV-VIS spectrophotometer at 368 nm. Drug loading content and encapsulation efficiency were calculated accordingly.

In vitro CPT-release of CPT-loaded nanoparticles

A typical procedure of in vitro release of the CPT from the nanoparticles was measured as follow: CPT-loaded three-layered nanoparticles (3LNPs/CPT) (3 ml, 0.59 mg/ml) prepared as described earlier were loaded in a dialysis bag ($MWCO = 3500$). The dialysis bag was immersed in 80 ml of DI water at pH 5.0 or 7.4 adjusted using HCl or Na_2CO_3. The temperature was kept at 37°C with horizontal shaking. At timed intervals, 8 ml of the medium outside the dialysis bag was withdrawn and the same volume of fresh DI water at the same pH was added to keep the total volume constant. The CPT concentration was determined by UV-Vis as described earlier.

Nanoparticle characterizations

The sizes of the nanoparticles were determined with the Nano-ZS Nanosizer. The polymer micelles were prepared as described earlier. The solution pH was adjusted to 5.0, 5.5, 6.0, 6.5, 7.0, or 7.5 using HCl or Na_2CO_3 before the measurements. The nanosizer was routinely calibrated with a 60-nm nanosphere™ size standard (Duke Scientific Corp. CA). Each measurement was performed in triplicate and the results were processed with DTS software Version 3.32.

The zeta potentials of the nanoparticles were determined using the phase analysis light scattering technology with the Nano-ZS Nanosizer routinely calibrated with a −50-mV zeta potential standard solution (Malvern Instruments). The nanoparticle concentration was 0.5 mg/ml. The measurements were performed in a disposable zeta capillary cell at 25°C with the attenuator set at 9 and F (Ka) value set at 1.5. Each measurement was performed for 30 runs.

Critical micelle concentration (CMC) of the copolymer was determined by our reported fluorescent method using N-phenyl-2-naphthylamine (PNA) as a fluorescent probe.[51] The fluorescent intensity was measured using a SPECTRAmax GEMINI XS spectrofluorometer (Molecular Devices). The excitation wavelength was 340 nm and the emission intensity at 418 nm was recorded with the cutoff wavelength at 420 nm.

The morphology and structure of the nanoparticles were observed using TEM according to the literature.[52] Typically, the specimen was prepared as follows. One drop of the nanoparticle solution was applied on a copper TEM grid covered with a very thin carbon film and dried at ambient temperature. A drop of 0.1 wt % phosphotungstic acid (PTA) or cisplatin aqueous solution was applied to the grid. After 3 min, the excess fluid was removed with a piece of filter paper. The sample grid was washed with water and dried at ambient temperature.

Drug distribution in the nanoparticle

Drug distribution was estimated using a fluorescent method with PNA as the fluorescence probe. PNA was loaded to the nanoparticle using the two- or one-step method from 1 ml of acetone solution containing terpolymer (2.5 mg) and PNA (2.19 μg, 10^{-8} mol).

Each nanoparticle solution was divided into two parts. One was adjusted to pH 7.4 and added with 0.6 mM $CuCl_2$, and the other was adjusted to pH 5 and added with 0.6 mM $CuCl_2$. The solutions' fluorescence intensities were measured using the SPECTRAmax GEMINI XS spectrofluorometer. The excitation wavelength was 340 nm and the emission intensity at 418 nm was recorded with the cutoff wavelength at 420 nm. The percent of PNA loaded in the PCL core was calculated as the ratio of fluorescent intensities of the solution at pH 5 with 0.6 mM $CuCl_2$ to that at pH 7.4 with 0.6 mM $CuCl_2$.

Cell culture

SKOV-3 adenocarcinoma cells were obtained from American Type Culture Collection. Cells were propagated to confluence in T-75 flasks (Corning Costar, Cambridge, MA) at 37°C under a humidified atmosphere of 5% CO_2 in 15 ml of RPMI-1640 medium with 10% fetal bovine serum (FBS), 10 μg/ml insulin, and 1% antibiotic/antimycotic solution (Sigma A9909). Cells were harvested from flasks with 0.25% trypsin/0.03% EDTA.

pH-dependent adsorption of 3LNPs onto the cell membrane

The attachment of the nanoparticles onto the cell membrane was observed using confocal laser scanning microscopy. The 3LNPs loaded with PKH26 (3LNPs/PKH26) were fabricated using the two-step method. SKOV-3 cells were cultured and harvested as described earlier. They were plated onto glass bottom Petri dishes (MatTek, Ashland, MA) at 80,000 cells per plate in 2 ml of RPMI-1640 medium (Sigma-Aldrich) supplemented with 10% FBS and incubated for 24 h at 37°C under a humidified atmosphere of 5% CO_2. After incubation the original medium was replaced with 1 ml of fresh medium at pH 6.0 or 7.4. Then, 20 μl of the 3LNPs/PKH26 solution (3LNP concentration was 0.5 mg/ml, PKH26 concentration was 5 μM) was added. The cells were incubated at 37°C for 15 min and then at 4°C for 15 min. The medium was removed and the cells were washed twice with cold PBS at 4°C. One ml of PBS was added to each dish and observed using the confocal microscope. Cells were kept at 4°C except when observed using the microscope.

A control experiment using the nanoparticle filtrate was carried out under the same conditions to test whether there was free PKH26 in the nanoparticle solution that dyed the cell membrane. The 3LNPs/PKH26 solution (1.6 ml) was filtered through a Centricon filter with a 3,000 molecular weight cutoff (Amicon, Bedford, Ma, no. YM-3) at 2600*g* for 1 h. Free dye should be in the filtrate while the nanoparticles should be retained on the filter. The filtrate was then applied to the cells and the cells were observed as described earlier. No fluorescence was observed in the cells.

Cellular uptake of the nanoparticles observed by confocal microscopy

SKOV-3 cells were plated onto glass bottom Petri dishes (MatTek, Ashland, MA) at 80,000 cells per plate in 2 ml of RPMI-1640 medium (Sigma-Aldrich) supplemented with 10% FBS. The plates were incubated for 24 h at 37°C in a humidified atmosphere of 95% air and 5% CO_2. The original medium was then removed and replaced with 1 ml of fresh medium at pH 6.0 or 7.4. The 3LNPs/PKH26 solution (20 μl, 3LNP concentration was 0.5 mg/ml, PKH26 concentration was 5 μM) was added. After 30 min, Lysotracker (Molecular Probes, Carlsbad, CA) was added to the wells at a concentration of 150 nM. Images were taken using a Leica TCS SP2 microscope after culturing for 2.5 h. Cells were kept at 37°C in a humidified atmosphere of 95% air and 5% CO2 except when observed on the microscope. Lysotracker was observed using a 488-nm laser and the emission wavelength was read from 510 to 540 nm and expressed as green. 3LNPs/PKH26 were observed using a 543-nm laser and the emission wavelength was read from 560 to 620 nm and expressed as red.

pH-dependent cellular uptake of 3LNPs measured by flow cytometry

The preparation of 3LNPs/PKH26 solution and its filtrate, and the cell culture and harvesting were as described earlier. Harvested cells were transferred into six-well plates (2.5-ml cell suspension/well at 2×10^5 cells/ml) and incubated for 24 h in a humidified atmosphere of 95% air and 5% CO_2. The original medium in each well was then replaced with 1 ml of medium containing the 3LNPs/PKH26 or the filtrate at 37°C at pH 6.0 or 7.4 for 4 h. The cells were washed with cold PBS twice. The cells were then collected using 0.5 ml trypsin solution (0.25% trypsin/0.03% EDTA) into eppendorfs containing 0.8 ml of PBS supplemented with 8% FBS and centrifuged at 1000*g* for 6 min at 4°C. The supernatant was removed and 1 ml of PBS with 2% FBS was added. The cells were then centrifuged again to remove the trypsin. The cells were resuspended in PBS with 2% FBS and kept at 0°C for analysis. The PKH26-positive cells and the average relative fluorescent unit were measured by flow cytometry. PKH26 was excited using an argon laser (488 nm) and the fluorescence at 590 nm was detected. Ten thousand gated events were collected and analyzed with the NPE Quanta™ 2.1 software program.

Hemolytic activity of the nanoparticles

All experiments were conducted with the approval of the University of Wyoming Animal Care and Use Committee. Mouse blood was collected in heparin containing eppendorf,

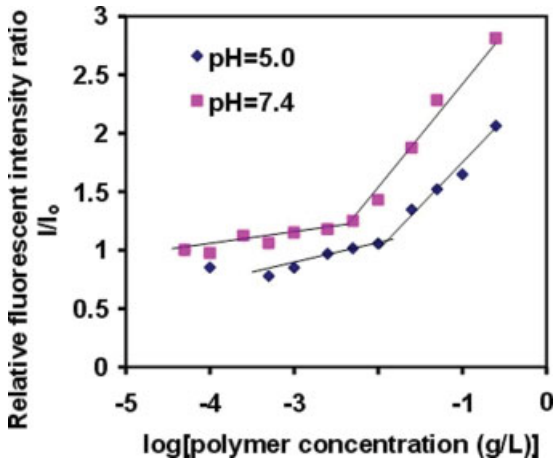

Figure 1. The PNA fluorescence intensity ratio I/I_0 as a function of log C of the terpolymer brush at pH of 5 and 7.4.

[PNA] = 1.0×10^{-6} M; (I/I_0 is the relative fluorescence intensity in the presence of PNA (I) and the absence (I_0) of PNA). [Color figure can be viewed in the online issue, which is available at www.interscience.wiley.com.]

and then centrifuged at 1000*g* for 5 min to separate the red blood cells (RBCs) from the plasma. The RBCs were dispersed in Alsexer's Buffer. The detailed hemolysis procedures were the same as we reported.[37] The hemolysis of RBCs in PBS solutions at pH 5.8 and 7.4 and in Milli-Q water was used as negative and positive controls. The observed hemolytic activity of 3LNPs at a given concentration and a pH value was normalized to that of the positive control using milli-Q water. All experiments were carried out in triplicates.

Results and Discussion

Design and synthesis of the terpolymer brush

The 3LNPs with a pH-responsive middle layer shown in Scheme 1 require a polymer with three types of polymer chains: hydrophobic polymer chains forming the core for carrying drug, PEG chains forming the outer layer for "stealth properties", and pH-responsive chains forming the pH-responsive middle layer. The known degradable nontoxic PCL was used as the hydrophobic chain. A tertiary amine-containing polymer PDEA, which is water insoluble at pH $>$ 6.5 but becomes soluble and positively charged at pH $<$ 6.5 by the protonation of the tertiary amine groups,[17] was used as the pH-responsive chain. Tertiary amine-containing polymers have relatively low toxicity.[53] Their toxicity is also related to their molecular weights. A lower molecular weight polymer has a lower toxicity.[54] To further decrease its toxicity, the molecular weight of PDEA was kept low, 2.5 KDa.

The polymer structure containing the three types of polymer chains was a terpolymer brush prepared by macromonomer copolymerization.[51] The methacrylic macromonomers of PEG, PCL, and PDEA (i.e., mPEG, mPCL, mPDEA) were prepared separately. Their molecular weights were optimized to be about 2 KDa to make the copolymer micelles about 100 nm in diameter. The macromonomers were copolymerized using free radical copolymerization as we reported.[51] The targeted brush copolymer is about 10 KDa, i.e., about 4–5 macromonomers connected together because high molecular weight polymer brushes have an extended chain structure[55] and may not be able to form micelles with diameters less than 100 nm. The copolymerization of the macromonomers at high initiator concentration (methacrylate units/AIBN molar ratio of 5) was found to produce a resulting terpolymer brush having a molecular weight of 10.8 KDa with a PDI of 1.8. The PCL/PDEA/PEG chain ratio was 0.90:1.0:1.9.

Fabrication of 3LNPs via pH-controlled hierarchical self-assembly

The fabrication of the 3LNPs is shown in Scheme 4. The terpolymer brush was firstly dispersed in a pH 5 solution. At this pH, the PDEA chains were protonated and became water soluble. The hydrophobic PCL chains (or with hydrophobic drug molecules) associated as the hydrophobic core with the PEG and protonated PDEA as the corona. After the solution pH was raised to 7.4, the PDEA chains were deprotonated and became hydrophobic, collapsing on the PCL core as a hydrophobic middle layer. The PEG chains formed the hydrophilic corona.

This stepwise formation of the nanoparticles was confirmed by measuring the CMCs of the terpolymer brush at pH 5 and 7.4 using PNA as a fluorescent probe (Figure 1). PNA has a high fluorescence activity in nonpolar environments, while polar solvents such as water can quench its fluorescence.[56] The CMC of the terpolymer was 15.8 mg/L at pH 5 and 4.0 mg/L at pH 7.4, indicating that at pH 5 the PDEA chains were indeed soluble, which led to a high CMC due to the presence of more water-soluble chains. At pH 7.4, the PDEA became hydrophobic and decreased the CMC.

The nanoparticles had a pH-dependent size and zeta potential, as shown in Figure 2. The nanoparticles were neutral at pH 7.4 but gradually became positively charged with decreasing the pH. This suggests that as the solution pH decreased, the PDEA chains became positively charged and soluble. Correspondingly, the nanoparticle hydrodynamic volume increased due to the electrostatic repulsion, as

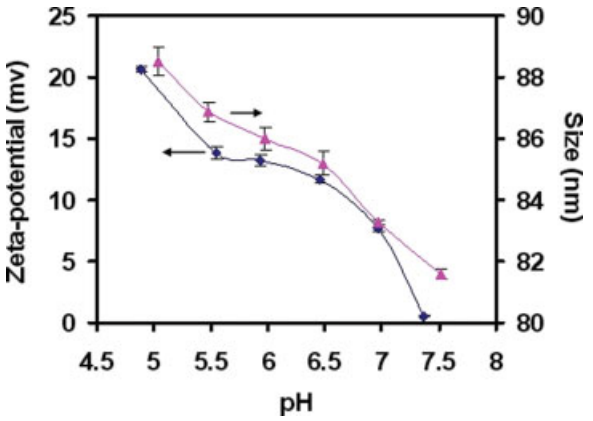

Figure 2. pH-Dependence of the size (▲) and zeta potential (●) of 3LNPs.

[Color figure can be viewed in the online issue, which is available at www.interscience.wiley.com.]

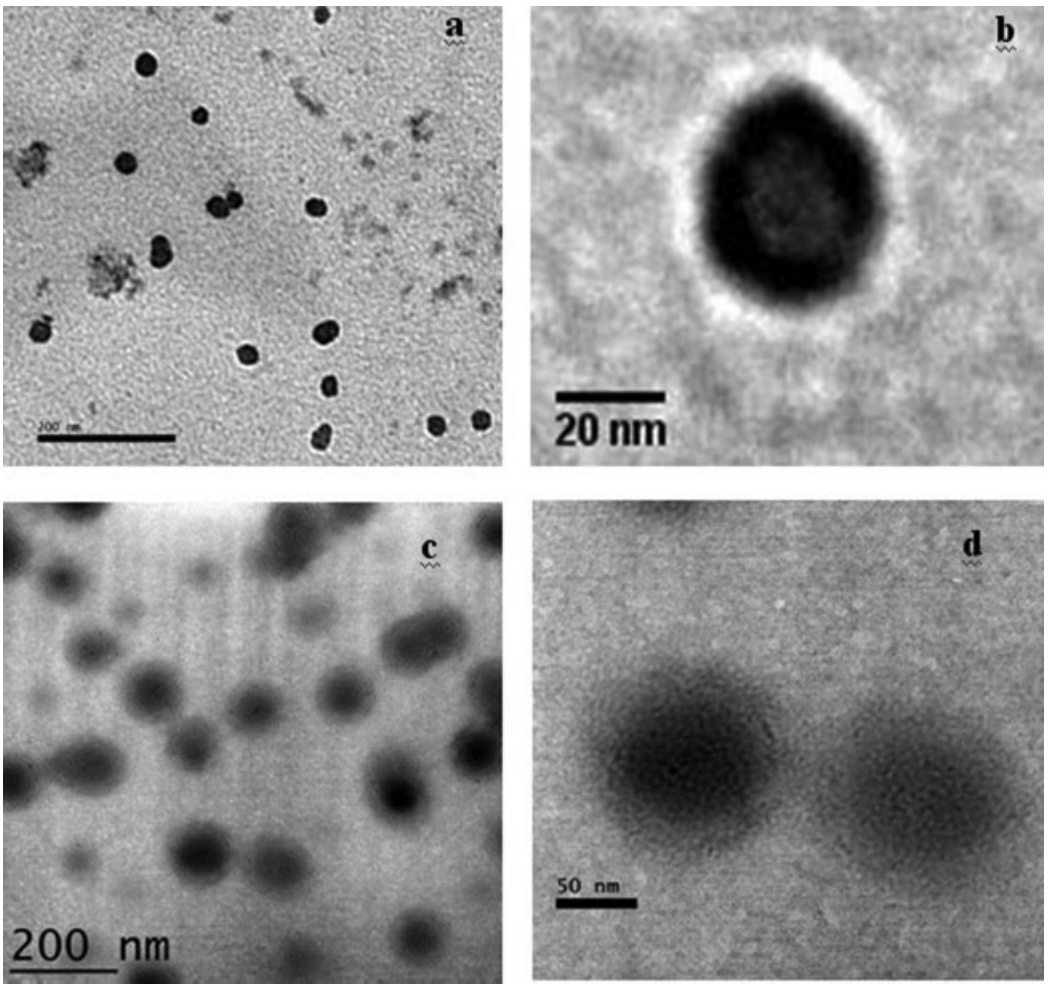

Figure 3. TEM images of 3LNPs made by the two-step method (a,b) and the nanoparticles by one-step method (c,d).

The PDEA chains were selectively stained by phosphotungstic acid or cisplatin.

confirmed by Figure 2. Increasing pH could remove the charges and the nanoparticles became smaller. Thus, the nanoparticles indeed can be reversibly positively charged as shown in Scheme 1.

The layered structures of the nanoparticles fabricated by two-step methods were further observed using TEM, as shown in Figure 3. The amine-containing PDEA can complex with PTA or cisplatin, and thus the PDEA layer can be selectively stained to enhance its contrast.[57] The images clearly revealed a three-layered spherical structure. The core was less dark because the electron beam traveled a shorter path through the PDEA layer. There was a darker PDEA layer surrounding the core. The diameter of the dry particles was about 60 nm with thickness of each layer estimated to be about 10 nm. This confirms that the hierarchical two-step self-assembly of the terpolymer brush indeed formed three-layered onion-structured nanoparticles. As a control, the nanoparticles fabricated by directly dropping the polymer solution into DI water (one-step method) had a two-layered core-shell structure (Figures 3c, d) (2LNPs). The homogeneously dark core indicates that the PDEA chains were mixed with the PCL chains in the core. The size of the 2LNPs was much larger than that of 3LNPs. This may be because of the loose packaging of the PCL and PDEA chains, which are immiscible.

Drug distribution in the nanoparticles

The burst drug release from nanoparticles is due to the drug molecules adsorbed on the nanoparticles surface and those loaded in the hydrophobic core but close to the hydrophilic surface. In the two-step fabrication, the hydrophobic PCL chains and drug (or a fluorescent dye) are expected to form the core first at pH 5. When the PDEA shell formed at pH 7.4, the drug (or dye) concentration in the solution already became lower. Thus, most of the drug (or dye) was expected to be loaded in the core of the 3LNPs. The distribution of a hydrophobic dye PNA in the 3LNPs was probed using a fluorescent quench method. For comparison, the drug distribution in the nanoparticles fabricated by the one-step method was also evaluated. Transition metal ions such as Cu^{2+} can quench the fluorescence of a dye such as PNA

Table 1. The Relative Fluorescence Intensity of PNA Loaded in the Nanoparticles at pH 7.4 or 5 in the Presence of $CuCl_2$

	3LNPs by Two-Step Method	2LNPs by One-Step Method
Conditions	Relative Fluorescent Intensity Ratio ($I/I_{pH7.4+Cu2+}$)	
pH 7.4 + Cu^{2+}	1	1
pH 5 + Cu^{2+}	0.84	0.43

$[PNA] = 1.0 \times 10^{-6}$ M, $[CuCl_2] = 0.6 \times 10^{-3}$ M.
The relative fluorescent intensity ratio was calculated using the fluorescence intensity of the nanoparticles at pH 7.4 in the presence of $CuCl_2$ (pH 7.4 + Cu^{2+}) as the reference.

contacting the aqueous solution. Thus, at pH 7.4 and in the presence of Cu^{2+}, the fluorescence came from the PNA in the PCL core and the PDEA middle layer. At pH 5, the PDEA layer became soluble, and thus in the presence of Cu^{2+}, the fluorescence came from the PNA in the PCL core only. Table 1 shows the relative fluorescence of the PNA-loaded nanoparticles solution in the presence of $CuCl_2$. About 84% PNA was in the PCL core of the 3LNPs prepared by the two-step method, while only 43% of PNA was loaded in the core of the core-shell structured 2LNPs prepared by the one-step method. Thus, the stepwise fabrication could load drugs more into the core.

This experiment using PNA as a probe and a model drug demonstrates the advantage of the two-step method in drug loading, and provides a qualitative guidance when loading other drugs to the nanoparticle. It should be advised that such properties of a drug as molecular weight, water solubility, and compatibility with the core of the nanoparticle can also affect its drug loading and should also be considered.

CPT-loading into the nanoparticles

CPT is a potent anticancer drug with a poor water solubility.[58] CPT was loaded into the nanoparticles by a solvent-displacement method. The CPT-loading efficiencies into the 3LNPs using the two-step fabrication was as high as 94.4 ± 3.9% with a drug content of 157.3 mg/g. The loading efficiency to the 2LNPs via the one-step method could only reach 60.7 ± 5.6%, similar to that of other core-shell micelles.[29] This comparison is agreeable with the drug distribution results and confirms that the 3LNPs made by the two-step fabrication method is more effective at encapsulating the hydrophobic drug.

The drug releasing profiles from the CPT-loaded 3LNPs and 2LNPs are shown in Figure 4a. CPT-release from the 3LNPs was pH-dependent: the CPT-release rate at pH 5 was

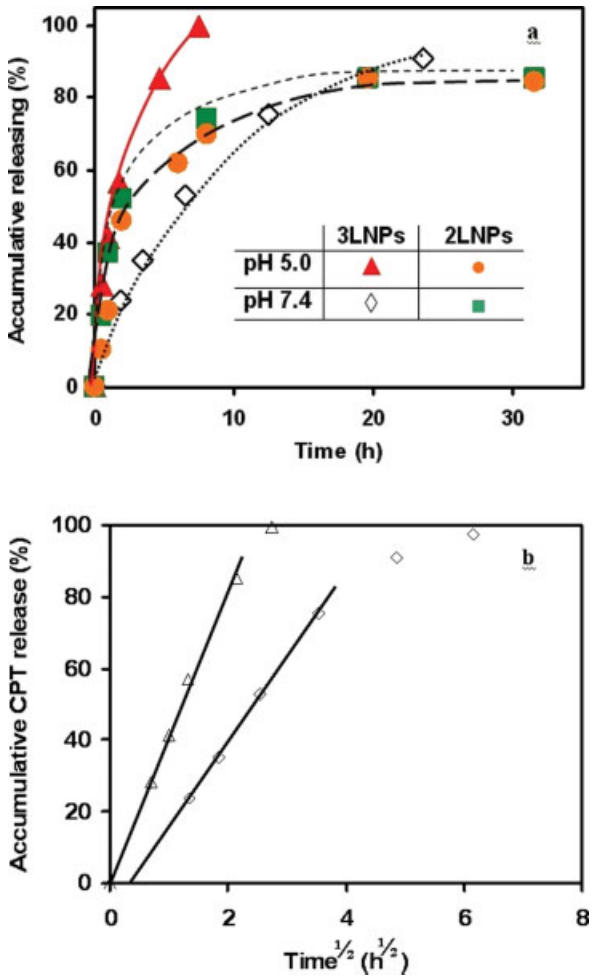

Figure 4. (a) CPT-release at pH 5 or 7.4 from CPT-loaded 3LNPs or 2LNPs at 37°C and (b) the accumulated CPT-release from the 3LNPs as a function of the square root of time at pH 5 (Δ) and 7 (◇).

[Color figure can be viewed in the online issue, which is available at www.interscience.wiley.com.]

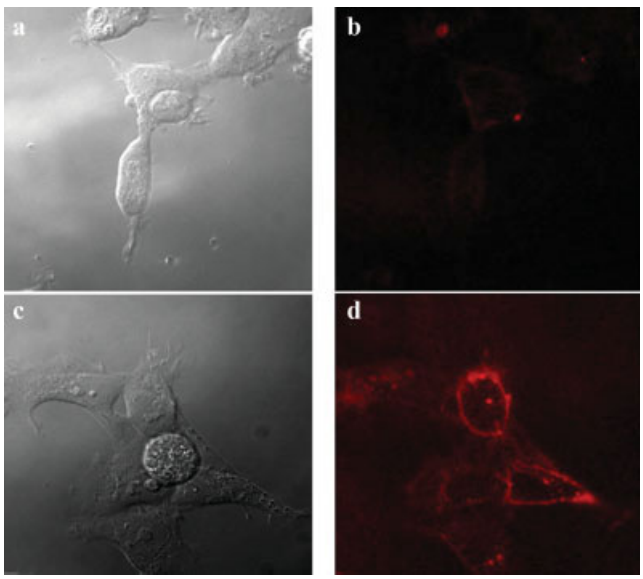

Figure 5. Adsorption of 3LNPs onto SKOV-3 cell membrane at pH 7.4 (a,b) and pH 6 (c,d) at 4°C observed with confocal microscopy.

Differential interference contrast (a,c), red PKH26 fluorescence channel (b,d); 3LNPs were loaded with PKH26. The 3LNP dose was 9.8 μg/ml. [Color figure can be viewed in the online issue, which is available at www.interscience.wiley.com.]

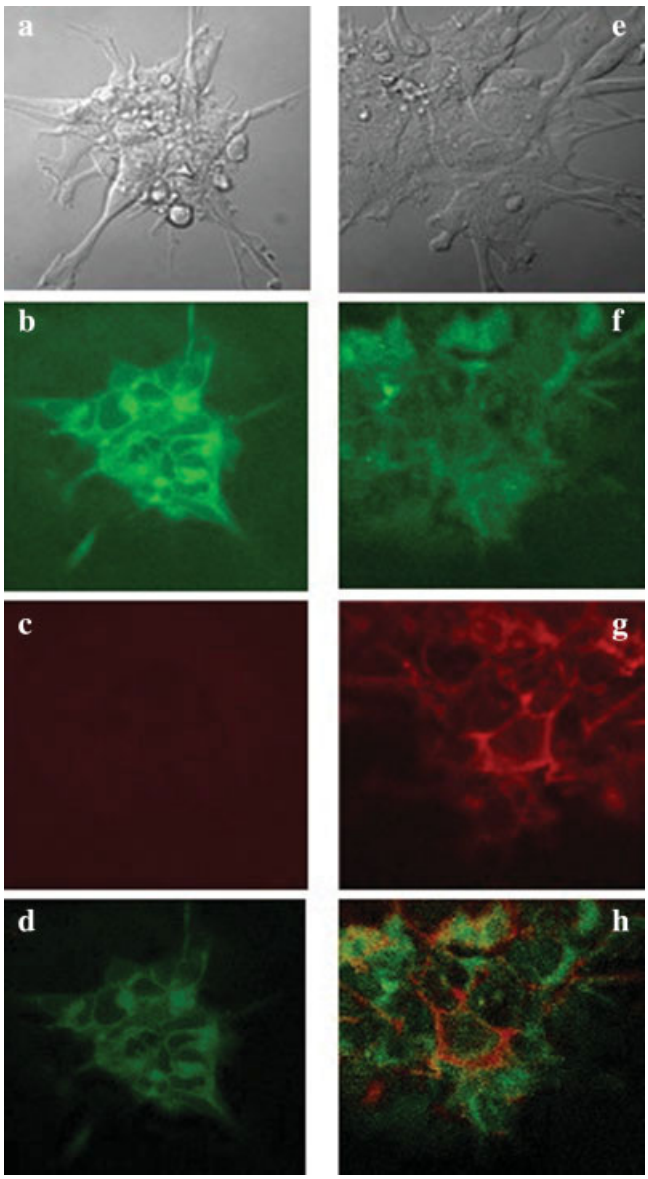

Figure 6. Confocal microscopy images of the cells observed with differential interference contrast (a,e), lysotracker (green) channel (b,f) (wavelength 510–540 nm), PKH26 (red) channel (c,g) (wavelength 560–620 nm), and the overlay of lysotracker and PKH26 images (d,h).

Cells were cultured at pH 7.4 (a, b,c,d) or 6 (e,f,g,h) with the 3LNPs/PKH26 for 2.5 h at 3LNP dose of 9.8 μg/ml. [Color figure can be viewed in the online issue, which is available at www.interscience.wiley.com.]

much faster than that at pH 7.4. The plots of accumulated CPT-release as a function of the square root of time at both pHs (Figure 4b) are linear up to 80%, suggesting that the CPT-release was a pure diffusion-controlled process without initial burst release.[59] There was about a 1.5 h delay in the CPT-release at pH 7.4 (Figure 4b). This was due to the protection of the PDEA-middle layer. On the contrast, the CPT release from the 2LNPs apparently, similar to other core-shell structures,[29] had a rapid burst release in the first several hours and the profiles at both pHs were almost the same, suggesting the lack of pH dependence. These results indicate that the PDEA-middle layer of the 3NLPs indeed provides a protection and inhibits the burst release of drug.

pH-dependent cellular uptake of the nanoparticles

The second designed function of the PDEA-middle layer of the 3LNPs is that at an acidic pH (e.g., solid tumor interstitial pH (<7)), the positively charged PDEA chains can lead the nanoparticles to be adsorbed on the negatively charged cell membrane to induce electrostatically adsorptive endocytosis. The effectiveness of the charged PDEA-induced adsorption on the cell membrane and subsequent cellular uptake of the 3LNPs were estimated using confocal microscopy. A hydrophobic dye PKH26 was loaded in 3LNPs as a tracer of the nanoparticles. The cells were cultured with the PKH26/3LNPs at 4°C for 15 min at pH 7.4 or 6. Figure 5 shows that the cells cultured with PKH26/3LNPs at pH 6 had bright red cell membranes, while those cultured at pH 7.4 were hardly visible. As a control, the cells cultured with the filtrate of PKH26/3LNPs had no fluorescence at all, suggesting that the fluorescence of the cells cultured with PKH26/3LNPs was not due to the free dye in the solution. We thus conclude that the 3LNPs are more easily attached to the cells at the low pH due to their positive charges.

Figure 6 shows the confocal microscopy images of the cells cultured with PKH26/3LNPs at pH 7.4 or 6 at 37°C for 2.5 h. Clearly, the cells cultured at pH 6 had much more PKH26/3LNPs compared with those cultured at the neutral pH. The internalized 3LNPs were localized in lysosomes marked with lysotracker (green). The cellular internalization of PKH26/3LNPs was also quantitatively measured by flow cytometry in terms of the percentage of PKH26-positive cells

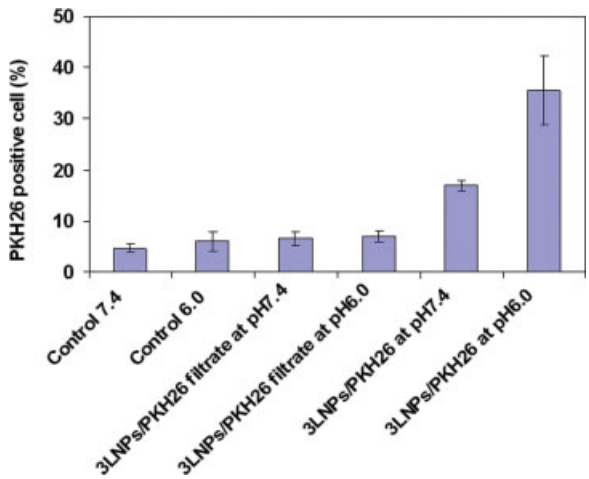

Figure 7. PKH26-positive cells determined by flow cytometry of cells cultured with 3LNPs/PKH26 solution at pH 7.4 and pH 6.0. SKOV-3 cells were cultured with the 3LNP solution or its filtrate for 4 h at 37°C.

Data are represented as a mean of three experiments and standard deviation. 3LNP dose was 23 μg/ml. [Color figure can be viewed in the online issue, which is available at www.interscience.wiley.com.]

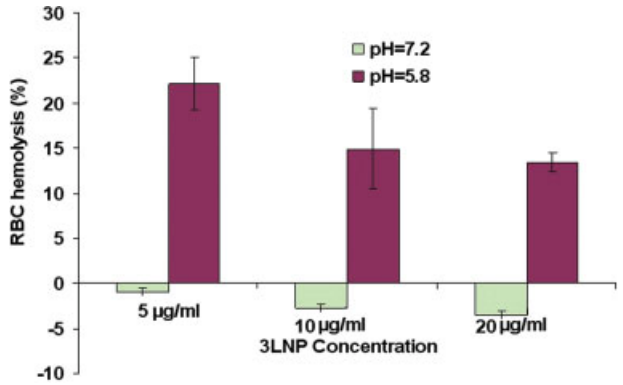

Figure 8. Mouse red blood cell hemolysis as a function of the 3LNP concentration at pH 7.2 or pH 5.8 at 37°C.

Data are represented as a mean of three experiments and standard deviation. [Color figure can be viewed in the online issue, which is available at www.interscience.wiley.com.]

(Figure 7). Consistent with the confocal microscopy results, a significantly more fraction of cells took up PKH26/3LNPs at pH 6 than that at pH 7.4 despite the fact that the cells at pH 6 were found not as active as those at pH 7.4. These results demonstrate that the 3LNPs are more easily taken up at pH 6 via electrostatically adsorptive endocytosis, which is consistent with the cell-membrane adsorption results (Figure 5).

Subcellular localization and lysosome escaping ability

As discussed in the Introduction section, drug release into the cytosol rather than into lysosomes is preferable to avoid drug sequestration and drug degradation.[44] Thus, the designed third function of the PDEA layer in the 3LNPs is to disrupt the lysosomal membrane to quickly release the internalized nanoparticles into the cytoplasm. In Figure 6, the overlapping of the images shows that some 3LNPs were localized in lysosomes or near lysosomes (yellow spots in Figure 6h). Some nanoparticles (red spots), however, were not in lysosomes, suggesting that they might have escaped from the lysosomes already. The ability of 3LNPs to disrupt lysosomes was estimated using RBCs hemolysis assay, which is widely used measure of the ability of a drug carrier to disrupt lysosomes.[60] The hemolytic activities of the 3LNPs at pH 5.8 and 7.2 were evaluated at 3LNP concentrations of 5, 10, and 20 μg/ml (Figure 8). A pH 5.8 rather than the lysosomal pH (4–5) was used because RBCs at pH 5 are not stable and easily lysed. At pH 7.2, the nanoparticle hardly lysed RBCs, but seemed to stabilize RBCs. While at pH 5.8, the 3LNPs quickly lysed about 15–20% RBCs within 1-h culture. One can estimate that the nanoparticle concentration in a 200-nm lysosome would be about 64 mg/ml even if the lysosome takes up only one 80-nm nanoparticle (assuming that the nanoparticle has an average density of 1 g/ml). This concentration is well-above the needed concentration for RBC hemolysis shown in Figure 8. In addition, at the lysosomal pH (~4–5), the PDEA layer of the 3LNPs was more positively charged (Figure 2). Thus, it can be concluded that 3LNPs could efficiently rupture the lysosomes for the nanoparticle escaping into the cytosol (red spots).

Conclusion

We demonstrate a new concept of a pH-controlled hierarchical self-assembly of PCL/PDEA/PEG terpolymer brush into layered nanoparticles with a pH-responsive PDEA middle layer that has multifunctions — inhibiting the premature burst drug release at the physiological pH, inducing electrostatically adsorptive endocytosis in the acidic solid tumor interstitium to greatly facilitate the cellular uptake of the nanoparticles, and disrupting lysosomal membrane for the nanoparticles to escape into cytosol. These active nanoparticles are promising as cancer drug delivery carriers.

Acknowledgments

The authors thank the financial supports from American Cancer Society (RSG-06-118-01-CDD), National Science Foundation (DMR-0705298), and National Institutes of Health (RR-016474).

Literature Cited

1. Sinha R, Kim GJ, Nie S, Shin DM. Nanotechnology in cancer therapeutics: bioconjugated nanoparticles for drug delivery. *Mol Cancer Ther*. 2006;5:1909–1917.
2. Brannon-Peppas L, Blanchette JO. Nanoparticle and targeted systems for cancer therapy. *Adv Drug Deliv Rev*. 2004;56:1649–1659.
3. van Vlerken LE, Amiji MM. Multi-functional polymeric nanoparticles for tumor-targeted drug delivery. *Expert Opin Drug Deliv*. 2006;3:205–216.
4. Yih TC, Al-Fandi M. Engineered nanoparticles as precise drug delivery systems. *J Cell Biochem*. 2006;97:1184–1190.
5. Sutton D, Nasongkla N, Blanco E, Gao J. Functionalized micellar systems for cancer targeted drug delivery. *Pharm Res*. 2007;24:1029–1046.
6. Rapoport N. Physical stimuli-responsive polymeric micelles for anticancer drug delivery. *Prog Polym Sci*. 2007;32:962–990.
7. Kwon GS. Diblock copolymer nanoparticles for drug delivery. *Crit Rev Ther Drug*. 1998;15:481–512.
8. Kataoka K, Harada A, Nagasaki Y. Block copolymer micelles for drug delivery: design, characterization and biological significance. *Adv Drug Deliv Rev*. 2001;47:113–131.
9. Brigger I, Dubernet C, Couvreur P. Nanoparticles in cancer therapy and diagnosis. *Adv Drug Deliv Rev*. 2002;54:631–651.
10. Moghimi SM, Hunter AC, Murray JC. Long-circulating and target-specific nanoparticles: theory to practice. *Pharmacol Rev*. 2001;53: 283–318.
11. Maeda H, Seymour LW, Miyamoto Y. Conjugates of anticancer agents and polymers: advantages of macromolecular therapeutics in vivo. *Bioconjug Chem*. 1992;3:351–362.
12. Jain RK. Delivery of molecular medicine to solid tumors: lessons from in vivo imaging of gene expression and function. *J. Control. Release*. 2001;74:7–25.
13. Yokoyama M, Okano T, Sakurai Y, Suwa S, Kataoka K. Introduction of cisplatin into polymeric micelle. *J. Control. Release*. 1996; 39: 351–356.
14. Uchino H, Matsumura Y, Negishi T, Koizumi F, Hayashi T, Honda T, Nishiyama N, Kataoka K, Naito S, Kakizoe T. Cisplatin-incorporating polymeric micelles (NC-6004) can reduce nephrotoxicity and neurotoxicity of cisplatin in rats. *Br J Cancer*. 2005;93:678–687.
15. Xu P, Van Kirk EA, Li S, Murdoch WJ, Ren J, Hussain MD, Radosz M, Shen Y. Highly stable core-surface-crosslinked nanoparticles as cisplatin carriers for cancer chemotherapy. *Colloi Surf B: Biointerf*. 2006;48:50–57.
16. Nishiyama N, Okazaki S, Cabral H, Miyamoto M, Kato Y, Sugiyama Y, Nishio K, Matsumura Y, Kataoka K. Novel cisplatin-incorporated polymeric micelles can eradicate solid tumors in mice. *Cancer Res*. 2003;63:8977–8983.
17. Xu P, Van Kirk EA, Murdoch WJ, Zhan Y, Isaak DD, Radosz M, Shen Y. Anticancer efficacies of cisplatin-releasing pH-responsive nanoparticles. *Biomacromolecules*. 2006;7:829–835.
18. Wong HL, Rauth AM, Bendayan R, Manias JL, Ramaswamy M, Liu Z, Erhan SZ, Wu XY. A new polymer-lipid hybrid nanoparticle

system increases cytotoxicity of doxorubicin against multidrug-resistant human breast cancer cells. *Pharm Res*. 2006;23:1574–1585.
19. Soppimath KS, Tan DC-W, Yang Y-Y. pH-triggered thermally responsive polymer core-shell nanoparticles for drug delivery. *Adv Mater*. 2005;17:318–323.
20. Hruby M, Konak C, Ulbrich K. Polymeric micellar pH-sensitive drug delivery system for doxorubicin. *J Control Release*. 2005;103: 137–148.
21. Gao ZG, Lee DH, Kim DI, Bae YH. Doxorubicin loaded pH-sensitive micelle targeting acidic extracellular pH of human ovarian A2780 tumor in mice. *J Drug Target*. 2005;13:391–397.
22. Lee ES, Na K, Bae YH. Doxorubicin loaded pH-sensitive polymeric micelles for reversal of resistant MCF-7 tumor. *J Control Release*. 2005;103:405–418.
23. Liang H-F, Chen S-C, Chen M-C, Lee P-W, Chen C-T, Sung H-W. Paclitaxel-loaded poly(g-glutamic acid)-poly(lactide) nanoparticles as a targeted drug delivery system against cultured HEPG2 cells. *Bioconjug Chem*. 2006;17:291–299.
24. Koziara JM, Whisman TR, Tseng MT, Mumper RJ. In-vivo efficacy of novel paclitaxel nanoparticles in paclitaxel-resistant human colorectal tumors. *J Control Release*. 2006;112:312–319.
25. Miura H, Onishi H, Sasatsu M, Machida Y. Antitumor characteristics of methoxypolyethylene glycol-poly(dl-lactic acid) nanoparticles containing camptothecin. *J Control Release*. 2004;97:101–113.
26. Williams J, Lansdown R, Sweitzer R, Romanowski M, LaBell R, Ramaswami R, Unger E. Nanoparticle drug delivery system for intravenous delivery of topoisomerase inhibitors. *J Control Release*. 2003;91:167–172.
27. Lamprecht A, Benoit JP. Etoposide nanocarriers suppress glioma cell growth by intracellular drug delivery and simultaneous p-glycoprotein inhibition. *J Control Release*. 2006;112:208–213.
28. Liu L, Li C, Li X, Yuan Z, An Y, He B. Biodegradable polylactide/poly(ethylene glycol)/polylactide triblock copolymer micelles as anticancer drug carriers. *J Appl Polym Sci*. 2001;80:1976–1982.
29. Zhang L, Hu Y, Jiang X, Yang C, Lu W, Yang YH. Camptothecin derivative-loaded poly(caprolactone-co-lactide)-b-PEG-b-poly(caprolactone-co-lactide) nanoparticles and their biodistribution in mice. *J Control Release*. 2004;96:135–148.
30. Yoo HS, Lee KH, Oh JE, Park TG. In vitro and in vivo anti-tumor activities of nanoparticles based on doxorubicin-PLGA conjugates. *J Control Release*. 2000;68:419–431.
31. Yokoyama M, Fukushima S, Uehara R, Okamoto K, Kataoka K, Sakurai Y, Okano T. Characterization of physical entrapment and chemical conjugation of adriamycin in polymeric micelles and their design for in vivo delivery to a solid tumor. *J Control Release*. 1998;50:79–92.
32. Kwon GS. Polymeric micelles for delivery of poorly water-soluble compounds. *Crit Rev Therap Drug Carrier Syst*. 2003;20: 357–403.
33. Laurand A, Laroche-Clary A, Larrue A, Huet S, Soma E, Bonnet J, Robert J. Quantification of the expression of multidrug resistance - related genes in human tumor cell lines grown with free doxorubicin or doxorubicin encapsulated in polyisohexylcyanoacrylate nanospheres. *Anticancer Res*. 2004;24:3781–3788.
34. Rapoport N. Combined cancer therapy by micellar- encapsulated drug and ultrasound. *Int J Pharm*. 2004;277:155–162.
35. Aouali N, Morjani H, Trussardi A, Soma E, Giroux B, Manfait M. Enhanced cytotoxicity and nuclear accumulation of doxorubicin-loaded nanospheres in human breast cancer MCF7 cells expressing MRP1. *Int J Oncol*. 2003;23:1195–1201.
36. Vauthier C, Dubernet C, Chauvierre C, Brigger I, Couvreur P. Drug delivery to resistant tumors: the potential of poly(alkyl cyanoacrylate) nanoparticles. *J Control Release*.93:151–160, 2003.
37. Xu P, Van Kirk E, Zhan Y, Murdoch WJ, Radosz M, Shen Y. Targeted charge-reversal nanoparticles for nuclear drug delivery. *Angew Chem Int Ed Engl*. 2007;46:4999–5002.
38. Torchilin VP, Trubetskoy VS. Which polymers can make nanoparticulate drug carriers long-circulating? *Adv Drug Deliv Rev*. 1995;16: 141–155.
39. Vittaz M, Bazile D, Spenlehauer G, Verrecchia T, Veillard M, Puisieux F, Labarre D. Effect of PEO surface density on long-circulating PLA-PEO nanoparticles which are very low complement activators. *Biomaterials*. 1996;17:1575–1581.
40. De. Jaeghere F, Allemann E, Feijen JK, T., Doelker E, Gurny R. Cellular uptake of PEO surface-modified nanoparticles: evaluation of nanoparticles made of PLA: PEO diblock and triblock copolymers. *J Drug Target*. 2000;8:143–153.
41. Savic R, Luo L, Eisenberg A, Maysinger D. Micellar nanocontainers distribute to defined cytoplasmic organelles. *Science*. 2003;300:615–618.
42. Barret A, Heath M. *Lysosomes: a Laboratory Handbook*, 2nd ed. New York: North-Holland, 1977.
43. Steinman RM, Mellman IS, Muller WA, Cohn ZA. Endocytosis and the recycling of plasma membrane. *J Cell Biol*. 1983;96:1–27.
44. Gong Y, Duvvuri M, Krise JP. Separate roles for the Golgi apparatus and lysosomes in the sequestration of drugs in the multidrug- resistant human leukemic cell line hl-60. *J Biol Chem*. 2003;278: 50234–50239.
45. Arancia G, Calcabrini A, Meschini S, Molinari A. Intracellular distribution of anthracyclines in drug resistant cells. *Cytotechnology*. 1998;27:95–111.
46. Engin K, Leeper DB, Cater JR, Thistlethwaite AJ, Tupchong L, McFarlane JD. Extracellular pH distribution in human tumours. *Int J Hyperthermia*. 1995;11:211–216.
47. Schmid S, Fuchs R, Kielian M, Helenius A, Mellman I. Acidification of endosome subpopulations in wild-type Chinese hamster ovary cells and temperature-sensitive acidification-defective mutants. *J Cell Biol*. 1989;108:1291–300.
48. Schmid SL, Fuchs R, Male P, Mellman I. Two distinct subpopulations of endosomes involved in membrane recycling and transport to lysosomes. *Cell*. 1988;52:73–83.
49. Reijngoud DJ, Tager JM. The permeability properties of the lysosomal membrane. *Biochim Biophys Acta.* 1977;472:419–449.
50. Lee ES, Na K, Bae YH. Super pH-sensitive multifunctional polymeric micelle. *Nano Lett*. 2005;5:325–329.
51. Xu P, Tang H, Li S-Y, Ren J, Van Kirk E, Murdoch WJ, Radosz M, Shen Y. Enhanced stability of core-surface cross-linked micelles fabricated from amphiphilic brush copolymers. *Biomacromolecules*. 2004;5:1736–1744.
52. Li X, Zuo J, Guo Y, Yuan X. Preparation and characterization of narrowly distributed nanogels with temperature-responsive core and pH-responsive shell. *Macromolecules*. 2004;37:10042–10046.
53. Verbaan FJ, Klouwenberg PK, van Steenis JH, Snel CJ, Boerman O, Hennink WE, Storm G. Application of poly(2-(dimethylamino)ethyl methacrylate)-based polyplexes for gene transfer into human ovarian carcinoma cells. *Int J Pharm*. 2005;304:185–192.
54. Wolf HK, de Raad M, Snel C, Steenbergen MJ, Fens MHAM, Storm G, Hennink WE. Biodegradable poly(2-dimethylamino ethylamino)-phosphazene for in vivo gene delivery to tumor cells. Effect of polymer molecular weight. *Pharm Res*. 2007;24:1572–1580.
55. Lee Hi, Jakubowski W, Matyjaszewski K, Yu S, Sheiko SS. Cylindrical core-shell brushes prepared by a combination of ROP and ATRP. *Macromolecules*. 2006;39:4983–4989.
56. You L, Lu F, Li Z, Zhang W, Li F. Glucose-sensitive aggregates formed by poly(ethylene oxide)-block-poly(2-glucosyl-oxyethyl acrylate) with concanavalin A in dilute aqueous medium. *Macromolecules*. 2003;36:1–4.
57. Lei L, Gohy J, Willet N, Zhang J, Varshney S, Jérôme R. Tuning of the morphology of core-shell-corona micelles in water. I. Transition from sphere to cylinder. *Macromolecules*. 2004;37:1089–1094.
58. Hatefi A, Amsder B. Camptothecin delivery methods. *Pharm Res*. 2002;19:1389–1399.
59. Higuchi T. Mechanism of sustained action medication: theoretical analysis of rate of release of solid drugs dispersed in solid matrices. *J Pharm Sci*. 1963;52:1145–1149.
60. Murthy N, Robichaud JR, Tirrell DA, Stayton PS, Hoffman AS. The design and synthesis of polymers for eukaryotic membrane disruption. *J Control Release*. 1999;61:137–143.

Manuscript received Sept. 27, 2007, revision received Feb. 14, 2007, and final revision received Jun. 20, 2008.